

### Discovery of Panguite, a New Ultra-Refractory Titania Mineral in Allende

Chi Ma<sup>1\*</sup>, Oliver Tschauner<sup>1,2</sup>, John R. Beckett<sup>1</sup>, Boris Kiefer<sup>3</sup>, George R. Rossman<sup>1</sup>, Wenjun Liu<sup>4</sup>; <sup>1</sup>Division of Geological and Planetary Sciences, California Institute of Technology, Pasadena CA 91125; <sup>2</sup>High Pressure Science and Engineering Center and Department of Geoscience, University of Nevada, Las Vegas, NV 89154; <sup>3</sup>Department of Chemical and Nuclear Engineering, University of New Mexico, Albuquerque, NM 87131; <sup>4</sup>Advanced Photon Source, Argonne National Laboratory, Chicago, IL 60439; \*chi@gps.caltech.edu.

**Introduction:** During our nano-mineralogy investigation of the Allende meteorite, we identified a new titania mineral named “panguite” in an ultra-refractory inclusion within an amoeboid olivine aggregate (AOA). It has an orthorhombic *Pbca* structure related to the *Ia3* bixbyite type and a formula unit  $(\text{Ti}^{4+}, \text{Al}, \text{Sc}, \text{Mg}, \text{Zr}, \text{Ca}, \square)_2\text{O}_3$ . We used electron probe microanalysis (EPMA), high-resolution scanning electron microscope (SEM), electron backscatter diffraction (EBSD), synchrotron micro-Laue diffraction with subsequent energy scans, and micro-Raman analyses to characterize the composition and structure. Panguite is not only a new mineral but also a new phase as synthetic *Ia3*  $(\text{Ti}^{4+}, \text{Al}, \text{Sc}, \text{Mg}, \text{Zr}, \text{Ca}, \square)_2\text{O}_3$  is not known. We report here the type occurrence of this new titania in nature and discuss implications of this phase for processes very early in the history of our solar system. The mineral and the mineral name (panguite) have been approved by the Commission on New Minerals, Nomenclature and Classification of the International Mineralogical Association (IMA 2010-057).

#### Occurrence, Chemistry and Crystallography:

Panguite occurs as small irregular to subhedral crystals (~0.5-2  $\mu\text{m}$ ) with Ti-rich davisite in an irregular ultra-refractory inclusion in Allende thick section Caltech MC2Q (Fig. 1). The refractory inclusion is about 30  $\mu\text{m} \times 20 \mu\text{m}$  in the section plane and resides within an AOA, surrounded by a matrix of mostly fine-grained olivine and troilite. Two compositionally distinct groups of panguite are observed in Allende MC2Q. The type panguite is Ti-, Sc-rich and Zr-, Y-poor and generally larger than Zr-rich panguite (smaller white grains in Fig. 2). We also observed panguite with perovskite, spinel and davisite in two other ultra-refractory inclusions in Allende.

The mean chemical composition of type panguite by EPMA is (wt%)  $\text{TiO}_2$  45.94,  $\text{ZrO}_2$  13.94,  $\text{Sc}_2\text{O}_3$  10.64,  $\text{Al}_2\text{O}_3$  8.28,  $\text{MgO}$  5.38,  $\text{Y}_2\text{O}_3$  4.91,  $\text{CaO}$  4.20,  $\text{SiO}_2$  3.37,  $\text{FeO}$  2.18,  $\text{V}_2\text{O}_5$  0.91,  $\text{Cr}_2\text{O}_3$  0.48,  $\text{HfO}_2$  0.09, sum 100.33. Repeated electron probe analysis of panguite with O measured gave similar results, implying that Ti in the structure is dominantly 4+. The Raman spectrum is also consistent with minimal  $\text{Ti}^{3+}$  being present based on comparisons with tistarite ( $\text{Ti}_2\text{O}_3$ ) and davisite. Assuming all Ti as  $\text{Ti}^{4+}$  leads to an empirical formula, based on 3 oxygens, of

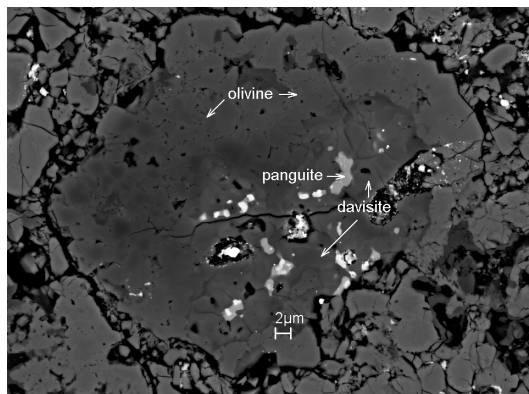


Fig. 1. SEM backscattered electron (BSE) image of the ultra-refractory inclusion in an Allende AOA.

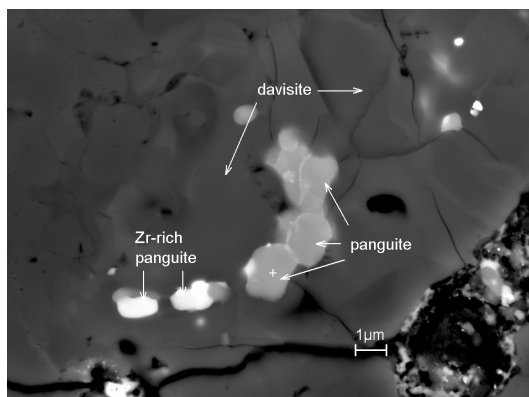


Fig. 2. Enlarged BSE showing the area where panguite crystals (type material) occur with smaller Zr-rich panguite in davisite (Fig. 1).

$[(\text{Ti}_{0.75}\text{Zr}_{0.15}\text{Si}_{0.07})^{4+}_{\Sigma 0.97}(\text{Al}_{0.21}\text{Sc}_{0.20}\text{Y}_{0.06}\text{V}_{0.02}\text{Cr}_{0.01})^{3+}_{\Sigma 0.5}(\text{Mg}_{0.17}\text{Ca}_{0.10}\text{Fe}_{0.04})^{2+}_{\Sigma 0.31}]_{\Sigma 1.78}\text{O}_3$  for type panguite with a general formula of  $(\text{Ti}^{4+}, \text{Al}, \text{Sc}, \text{Mg}, \text{Zr}, \text{Ca})_{1.8}\text{O}_3$ , or  $(\text{Ti}^{4+}, \text{Al}, \text{Sc}, \text{Mg}, \text{Zr}, \text{Ca}, \square)_2\text{O}_3$ . Associated Zr-rich panguite (Fig. 2) has an empirical formula  $[(\text{Ti}_{0.55}\text{Zr}_{0.28}\text{Si}_{0.15})^{4+}_{\Sigma 0.98}(\text{Al}_{0.14}\text{Sc}_{0.12}\text{Y}_{0.12}\text{Cr}_{0.01}\text{V}_{0.01})^{3+}_{\Sigma 0.40}(\text{Ca}_{0.20}\text{Mg}_{0.15}\text{Fe}_{0.09})^{2+}_{\Sigma 0.44}]_{\Sigma 1.82}\text{O}_3$  and host davisite  $(\text{Ca}_{0.96}\text{Mg}_{0.04})_{\Sigma 1.00}[(\text{Sc}_{0.34}\text{Ti}_{0.23}\text{Y}_{0.01}\text{V}_{0.01}\text{Al}_{0.01})^{3+}_{\Sigma 0.60}(\text{Mg}_{0.23}\text{Fe}_{0.05})^{2+}_{\Sigma 0.28}(\text{Ti}_{0.08}\text{Zr}_{0.04})^{4+}_{\Sigma 0.12}]_{\Sigma 1.00}(\text{Si}_{1.12}\text{Al}_{0.83}\text{Ti}^{4+}_{0.05})_{\Sigma 2.00}\text{O}_6$ , where  $\text{Ti}^{3+}$  and  $\text{Ti}^{4+}$  are partitioned based on stoichiometry. Note that most of the Ti in davisite coexisting with the panguite, is trivalent. Small crystals of Ru-Ir-Mo-Fe-Os alloys are included in small amounts in davisite, or in contact with panguite. The surrounding olivine is  $\text{Fa}_{21}\text{Fo}_{79}$ .

EBSD patterns of panguite can not be matched against the structures of tistarite, perovskite,  $Ti_3O_5$ ,  $Sc_2TiO_5$ , armalcolite, pseudobrookite, anatase, rutile, or brookite. They do imply a  $CaF_2$ -type structure, which assisted us in identifying its bixbyite-related structure (a defect form of the  $CaF_2$  structure) by synchrotron analysis.

Synchrotron micro-Laue-diffraction on one panguite grain was carried out at the 34ID-E undulator beamline of the Advanced Photon Source in the Argonne National Laboratory using a  $0.5 \times 0.5 \mu m^2$  polychromatic X-ray beam. An energy scan by synchrotron mono-beam yielded a set of 17 reflections whose Q-values indicate an orthorhombic distortion of the cubic cell proposed by the EBSD patterns. Moreover the Q-values of these reflections imply a unit cell larger than that of fluorite. Related structure types with larger unit cells, which are common among anion-deficient fluorite-type structures, are the pyrochlore and the bixbyite type. We modelled orthorhombic distorted fluorite-, pyrochlore- and bixbyite cells of panguite using subgroups of the cubic aristotype cells and found a match of all reflections only for the bixbyite type in space group *Pbca*. Trial indexing with Jade 6.5 also indicated cell shapes compatible with a primitive orthorhombic distorted bixbyite-type cell.

Based on the indices from trial indexing and subsequent cell refinement using the program UnitCell, we evaluated the observed and calculated structure factor moduli and found agreement with a  $R_{int}$  of 6.1%. The observed structure factors show no evidence for ordering of cations among the four available sites. The orthorhombic distorted bixbyite cell of panguite was used to calculate an EBSD pattern and compared to the observed patterns. The EBSD patterns can be indexed nicely by the *Pbca* structure.

Panguite has a cation-deficient *Pbca* structure related to the *Ia3* bixbyite group, showing a unit cell:  $a = 9.781(1) \text{ \AA}$ ,  $b = 9.778(2) \text{ \AA}$ ,  $c = 9.815(1) \text{ \AA}$ ,  $V = 938.7(1) \text{ \AA}^3$  and  $Z = 16$ .

**Origin and Significance:** Zr is a key element in deciphering some of the earliest and most extreme environments before and during formation of the solar system because its oxide is highly refractory in both reducing and oxidizing gases [1] and it holds isotopic clues to nucleosynthetic contributions to the solar system and how they were introduced [2]. A variety of Zr, Y, Sc rich oxides and silicates, including allendeite, tazheranite, panguite, and davisite, have been reported in refractory inclusions [3-7] but only recently, with the advent of new microanalysis techniques, has it become possible to characterize these phases well enough to justify their possible use in placing quantita-

tive constraints on origin. Panguite is particularly interesting as a potential sensor of environment because it is a titanate that contains significant concentrations of Al (ionic radius in octahedral coordination of  $0.48 \text{ \AA}$ ), Sc ( $0.73 \text{ \AA}$ ), and Y ( $0.89 \text{ \AA}$ ), so it should also be able to readily accept large concentrations of  $Ti^{3+}$  ( $0.67 \text{ \AA}$ ). The absence of measurable  $Ti^{3+}$  in our Allende panguite therefore strongly suggests that these crystals equilibrated in a highly oxidizing environment. Yet they coexist with davisite that has  $Ti^{3+}/Ti^{4+} \sim 2$ , strongly suggesting very reducing conditions. This intimate juxtaposition of highly oxidized and highly reduced phases (Fig. 2) is thematically similar to the presence in type B inclusions of  $Ti^{4+}$ -enriched spinels hosted by  $Ti^{3+}$ -enriched clinopyroxene [8]. Zr-Y-Sc enriched phases are, however, likely to provide more direct clues to the source of extravagant dichotomies in redox conditions because they contain many more independent constraints on their environment.

Panguite is more than 20% higher in density than tistarite, the other  $Ti_2O_3$ -polymorph found in Allende [9]. This suggests formation of panguite may have formed at high pressure and opens the interesting possibility that panguite formed during a very early shock event potentially prior to encapsulation in the CAI. We examined this possible high pressure origin by ab initio calculations. Our results indicate that the stable high pressure form of  $Ti_2O_3$  is not the panguite- but the  $Th_2S_3$ -structure [10]. However, among all plausible  $A_2O_3$ -structures, panguite-type  $Ti_2O_3$  has the lowest  $\Delta H$  compared to tistarite at ambient and to  $Th_2S_3$ -type  $Ti_2O_3$  at elevated pressure. Therefore, if panguite is a high pressure phase, it either formed directly from condensation at elevated pressure because of a low seed-formation energy consistent with the Oswaldt-rules, or upon high-temperature release out of the  $Th_2S_3$ -type structure. Finally, it is possible that panguite formed at low pressures due to stabilization by solution of Sc, Al, Ca, Mg, and REE. We will examine these possibilities by static and dynamic compression experiments.

**References:** [1] Lodders K. (2003) *App. J.* 591, 1220. [2] Nicolussi et al. (1997) *Science* 277, 1281. [3] Allen J.M. et al. (1980) *GCA* 44, 685. [4] Hinton R.W. and Davis A.M. (1988) *GCA* 52, 2573. [5] El Goresy A. et al. (2002) *GCA* 66, 1459. [6] Ma C. et al. (2009) *LPSC* Abstr. # 1402. [7] Ma C. and Rossman G.R. (2009) *Am. Min.* 94, 845-848. [8] Paque J.M. et al. (2010) *LPSC* Abstr. # 1391. [9] Ma C. and Rossman G.R. (2009) *Am. Min.* 94, 841-844. [10] Nishio-Hamane D. et al. (2009) *High Pressure Res.* 29, 379-388.